Journal of Sound and Vibration (1999) **226**(2), 383–396
Article No. jsvi.1999.2225, available online at http://www.idealibrary.com on IDEAL®

AN EXPERIMENTAL STUDY ON THE NOISE CHARACTERISTICS OF NOTCHED CIRCULAR-SLOT JETS

S. B. VERMA AND E. RATHAKRISHNAN

Department of Aerospace Engineering, Indian institute of Technology, Kanpur - 208 016, *India*

(*Received* 7 *July* 1998, *and in final form* 23 *February* 1999)

1. INTRODUCTION

Jet characteristics are most receptive to changes in initial conditions, which play a dominant role in the development of both low [1–3] and high-speed [4] jets. From the literature it is seen that jets from non-circular geometries [1–3, 5, 6] result in enhanced mixing, a characteristic making them far superior to the conventional circular jet. This is attributed primarily to the axis-switching phenomenon caused by the non-uniform self-induction process predominant in the development of these jets [6]. Further, improvement of jet flow field in non-circular jets was achieved by Schadow *et al.* [1] in triangular and square nozzle jets wherein the small-scale eddies shed from the corners interact strongly with the large-scale vortices shed from the plain sides. Some similar observations have been made for rectangular-slot jets [3, 7].

Flows from modified circular/axisymmetric nozzles have been studied by a number of investigators. Gross distortions in the jet structure have been observed using intrusive means in circular jets, e.g., tabs both in subsonic [8] and supersonic regimes [9] which introduce gross distortions in the jet flow field and bring about increase in entrainment. In supersonic jets, tabs help to weaken the shock structure considerably and, hence, reduce the overall jet noise [10–12]. Non-intrusive means were also explored by Pannu and Johanneson [13] using triangular notches in a conical circular nozzle. The study revealed a much higher spread in the notched plane with the shedding of vortices from the edges of the notches. This vortical structure was found by them to act as a shielding device to the shock structure resulting in noise reduction. Norum [11] and McDaniel *et al.* [14] used fingers/slots in the nozzle parallel to the jet axis. The pressure relieving effect of the fingers/slots greatly weakens the shock structure and hence, reduces shock-associated noise.

The present study aims at understanding the changes introduced by the presence of notches in a circular-slot jet for the purpose of mixing enhancement and noise reduction. The source of noise has been reported by Hammitt [15], Glass [16] and McDaniel *et al.* [14] to be located approximately at the end of the third shock cell, and as such relieving the excess pressure through notches may help weaken the

0022-460X/99/370383 + 14 $30.00/0

shock structure and reduce the noise of sonic underexpanded circular-slot jets. No work seems to have reported the effect introduced by notch geometry variation on the mixing and noise characteristics of sonic underexpanded circular-slot jets.

2. EXPERIMENTAL SET-UP AND PROCEDURE

The experiments were conducted using a high-speed jet facility which consists of a cylindrical settling chamber, containing three mesh screens set 3 cm apart for minimizing the disturbance level and fluctuations at the slot inlet and connected to high pressure storage tanks. The desired slot geometry was carved on circular aluminium plates of 1·3 mm thickness and fixed perfectly to the end of the settling chamber using an O-ring so as to ensure no leakage even at very high settling chamber pressure. The area ratio between the settling chamber end-plate and slot was 100. The settling chamber pressure P_0, which was the controlling parameter in our investigation, was regulated using a pressure regulating valve. All the pressure measurements were made using long U-tube mercury manometers.

To study the effect of notch geometry alone on jet development, jets issuing from slots were preferred. However, it is to be mentioned that the slots used for the present study are not "sharp-edged" as used by Hussain and Husain [6] but are 'square-edged', called "*disk nozzle*" [17]. Such "*disk nozzles*" were found by Husain and Ramjee to be free from the effects of *vena-contracta*. Further, the slots have negligible boundary layer growth in them and as such have similar initial conditions, and hence can be used for comparative study of mixing characteristics from varying slot geometries [17]. The use of orifices instead of nozzles is justified by Gutmark and Schadow [18], who have shown that an elliptic slot jet of aspect ratio 3 : 1 has large and small-scale characteristics similar to an elliptic jet with well-designed contraction. This feature is important for engineering applications where the simplicity of slot design, especially with non-circular geometries, is advantageous [18].

The modifications in the circular slots consist of two notches placed symmetrically along the diameter as shown in Figure 1. Here the Y-axis is taken along the notched plane and the Z-axis along the unnotched plane of modified circular slot. Each notch conforms to 5% of the total plain circular slot area. All the slots, i.e., plain and modified, were of equal area, which was equal to the area of a circular slot of 10 mm diameter and thus the equivalent diameter, D_e, of the modified slots was 10 mm. Three notch configurations, namely semi-circular, square and triangular (vertex angle 60°) were investigated. Figure 1 shows a schematic diagram of the slot mounting attachments and the model used.

The investigation was carried out for two conditions: (1) correctly expanded sonic jets, $M_j = 1{\cdot}0$ and (2) underexpanded sonic jets at P_0/P_a of 7·82, $M_j = 2{\cdot}0$, corresponding to a level of underexpansion of 4·14. The Reynolds number based on the equivalent diameter and the equivalent exit velocity (based on M_j, which is defined as the Mach number obtained by correctly expanding the underexpanded jet) for the two conditions ranged from $2{\cdot}36 \times 10^5$ to $4{\cdot}72 \times 10^5$. All the tests were carried out at a room temperature of 30°C and 730 mmHg of pressure averaged

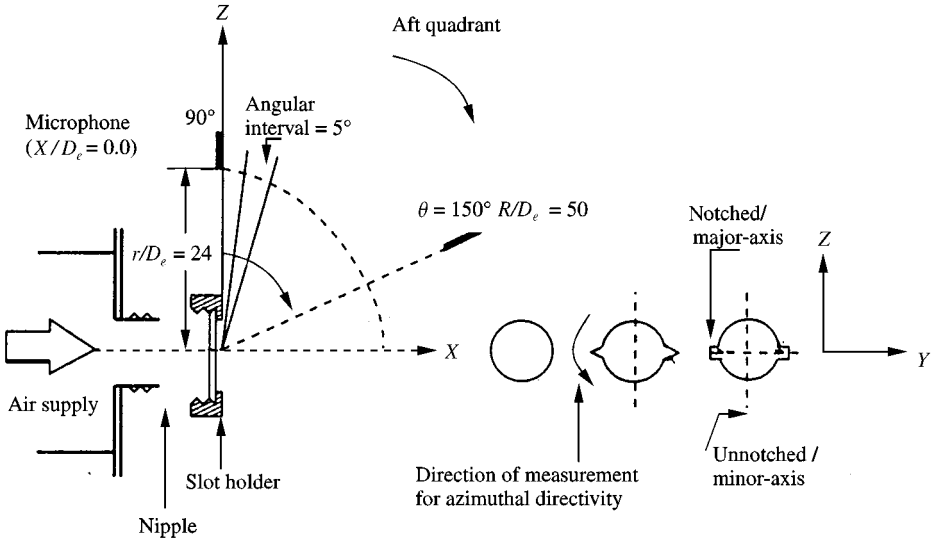

Figure 1. Schematic diagram of slot attachments and mountings, models and various measurement planes.

over the time taken for the completion of experiments. The variation in temperature was less than 0·1% and that for pressure about 2%.

Measurement techniques: The sensing probe used for obtaining mean flow measurements of the flowfield for the present investigation was a Pitot tube with an outer diameter of 0·55 mm. In all the measurements the sensing probe was oriented parallel to jet X-axis. The accuracy of traverse movement along X, Y, and Z directions was ± 0.1 mm. All the pressure measurements were accurate up to ± 1 mm of mercury column and were found to be repeatable within $\pm 3\%$. The grid data was taken on one side (i.e., a quadrant) and extended to the whole folwfield assuming symmetry of flowfield about Y and Z-axis.

The noise measurements were carried out in a jet acoustic chamber ($3 \times 2 \times 2$ m) which satisfied anechoic condition frequencies of 660 Hz and above. A Larsen and Davis 800B Model sound level meter with a $\frac{1}{8}$ in microphone was used to obtain the OASPL measurements. The microphone was calibrated using a Larsen and Davis CA250 calibrator with corrections for day-to-day changes in atmospheric pressure. The accuracy, according to the manufacturers specifications, was within $\pm$ 0·3 dB in the range of 20 Hz–20 kHz. Figure 1 shows the various measurement planes and microphone location for the present investigation.

Measurement of average shock-cell length has been carried out using a simple non-intrusive technique. A sharp-tipped pointer was attached to the traversing system and positioned in such a way that it was exactly at the slot exit plane, but sufficiently away from the flowfield so as not to be of any disturbance. The shadowgraph images of the underexpanded jets were captured on a screen along with the pointer. The angle made by the light source with the parallel beam reflected from the mirror was kept less than 5° ensuring proper accuracy of

quantitative measurement of shock-cell length using shadowgraph images in conjunction with the pointer and traverse arrangement. The pointer was moved parallel to the jet axis from the beginning of each shock cell to its end with the movement of the pointer being constantly monitored on the screen. The distance travelled by the pointer up to the fourth cell was measured by the movement of the traverse. Knowing the total length of four repetitive cells the average shock-cell length. L_{avg}, was calculated. The shock-cell length measured was accurate upto $\pm 2\%$. The repeatability of the noise and shock-cell measurements was within ± 2 and $\pm 3\%$ respectively.

3. RESULTS AND DISCUSSIONS

3.1. ISO-VELOCITY CONTOURS

Figures 2(a–d) show the iso-velocity contours for a plain circular slot jet as it develops in a cross-sectional plane in the downstream direction. In these plots the local flow velocity 'U' is normalized by the local centreline velocity 'U_c'. The measured pitot pressures, P_t, are reduced to velocities by using the relation

$$M = \sqrt{\left\{5\left[\left(\frac{P_s}{P_t}\right)^{-0\cdot2857} - 1\right]\right\}}.$$

This expression is nothing but a conveniently modified form of the well-known isentropic relation

$$P_t/P_a = \left(1 + \frac{\gamma - 1}{2} M^2\right)^{\gamma/(\gamma-1)}.$$

Note that this relation is used with the assumption that $\gamma = 1{\cdot}4$ and that the local static pressure, P_s, inside the jet could be approximated by the ambient pressure, P_a. The figures show smooth contours indicating the absence of any discontinuity in either the X–Y or X–Z planes.

Figures 3(a–d) show the iso-velocity contours for the triangular notched/modified circular slot jet at $M_j = 1{\cdot}0$. The presence of the notch in circular slot introduces a slight aspect-ratio in the modified circular slot. Designating the notched/modified (X–Y) plane as the major-axis plane and the unmodified (X–Z) plane as the minor-axis plane of the modified circular geometry, as shown in Figure 3(e), it is observed in Figure 3(a, b) that at $X/D_e = 5{\cdot}0$, the two axes interchange/switch, i.e., the initial (designated) major-axis becomes the new minor-axis and *vice versa*. In other words, axis switching is observed as is typical of jets issuing from non-circular exit geometries. The above process is illustrated through Figure 3(e) showing the cartoon of the cross-sectional growth of the modified circular or equivalent elliptic jet. Axis switching was also observed for semi-circular and square notch configurations (results are not presented here). This feature is totally absent in plain circular-slot jet owing to symmetry of geometry about the jet

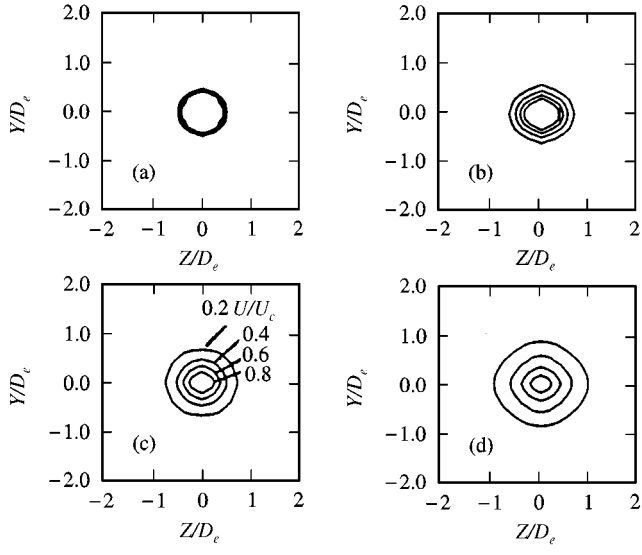

Figure 2(a–d). Iso-velocity contours for plain circular-slot jet at $M_j = 1{\cdot}0$. (a) $X/D_e = 0{\cdot}5$; (b) $X/D_e = 2{\cdot}0$; (c) $X/D_e = 5{\cdot}0$; (d) $X/D_e = 8{\cdot}3$.

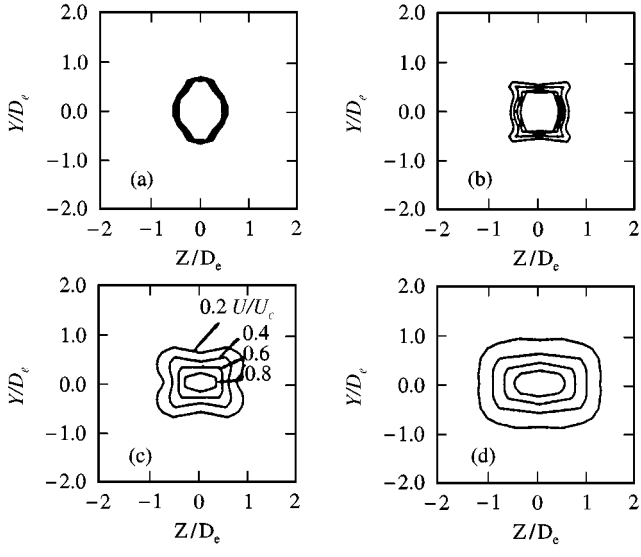

Figure 3(a–d). Iso-velocity contours for triangular notched circular-slot jet at $M_j = 1{\cdot}0$. (a) $X/D_e = 0{\cdot}5$; (b) $X/D_e = 2{\cdot}0$; (c) $X/D_e = 5{\cdot}0$; (d) $X/D_e = 8{\cdot}0$.

axis (Figure 2). The sharper curvature at the location of the notch relative to the remaining portions of the slot seems to result in the local bending of the vortex, and hence causes self-induced azimuthal deformations which is responsible for axis-switching and enhanced mixing in non-circular jets [16].

Hussain and Husain [6] attribute the comparatively reduced growth of the jet along the major-axis plane to the deformation of non-circular vortical structures. The explanation given is that the extremely thin initial boundary layer in slot jets

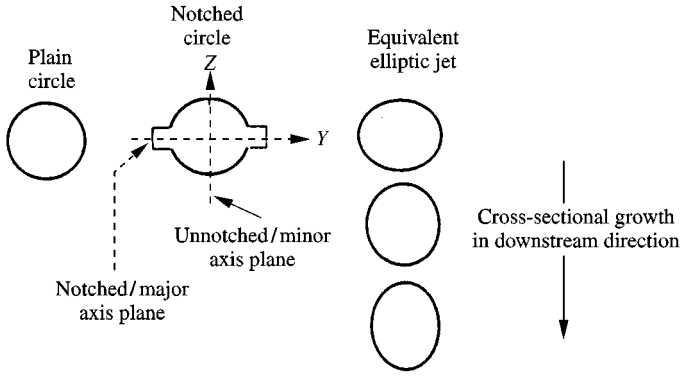

Figure 3(e). Cartoon showing the cross-sectional growth a notched circular-slot jet.

produces slender vortical structures with very thin cores (thus high vorticity) and with strong azimuthal variations in induced velocity. The self-induced velocity of a curved vortex filament [6] is

$$u = b_n \frac{\kappa}{4\pi\rho} \ln \frac{\rho}{\sigma},$$

where κ is the vortex strength (i.e., circulation), ρ is the radius of curvature, σ is the core radius and b_n is the local unit vector in the direction of the binormal. This azimuthal variation of induced velocity results in the deformation of the convecting vortex structures and consequent axis switching which is responsible for enhanced overall mixing.

3.2. CENTRELINE PRESSURE DECAY

Figure 4 shows the decay of centreline pressure with axial distance for the four cases investigated at $M_j = 1{\cdot}0$. A faster centreline pressure decay is usually a reasonable measure of faster jet spread [8, 9]. Also, it has been observed by Roshko [19] that the breakdown of the large-scale structures into fine-scale structures begins at the end of the potential core and this is seen as a drastic decay in the centreline pressure [5].

It is seen from the plot (Figure 4) that the potential core length for all the cases is almost unchanged suggesting that the growth of the shear layer in this region is not influenced by the presence of notches. Thereafter, the notched jets decay faster than the plain cases which have the least decay followed by triangular, square and finally by semi-circular notched jet which has the maximum decay. This is suggestive of the faster cascade of large structures into small scales for notched jets relative to plain case in accordance to the observations of Steiger *et al.* [5]. To verify the above case, pitot surveys across the shear layer were made. Figures 5 and 6 show the results so obtained for plain and notched jets respectively. It is clearly seen from the pressure profiles in the notched and unnotched planes, as shown in Figures 6 (a, b),

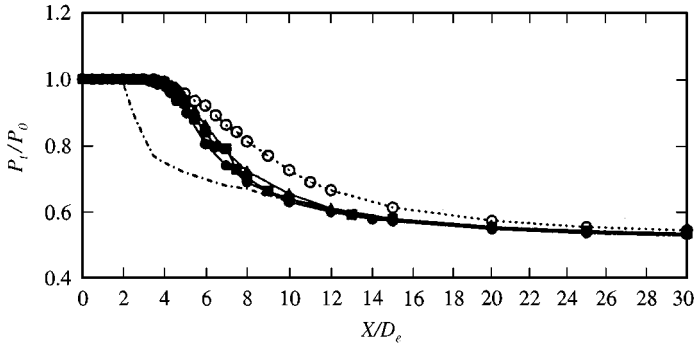

Figure 4. Centreline pressure decay comparison for varying notch geometry at $M_j = 1{\cdot}0$. - - - - - - - - Samimy *et al.*, 1993; ……. ○ …… Plain circle; ——▲—— Notch: Triangular; ——■—— Square; ——●—— Semi-circular.

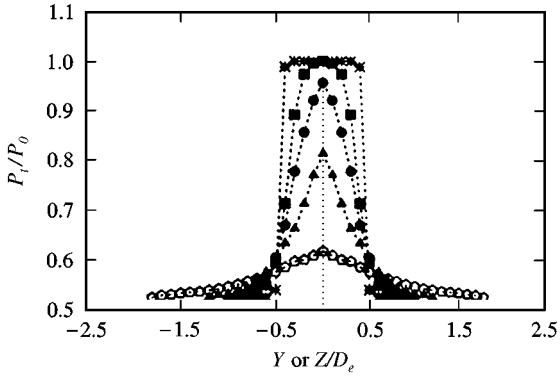

Figure 5. Pressure profiles for plain circular slot jet, $M_j = 1{\cdot}0$.

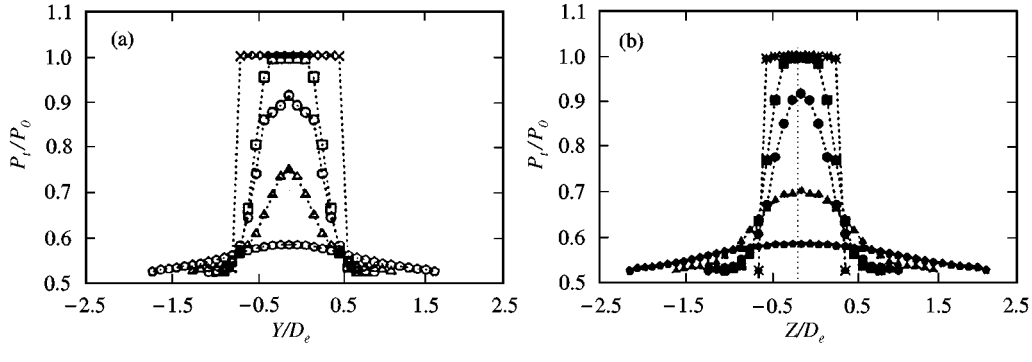

Figure 6. Pressure profiles for square notched circular slot jet, $M_j = 1{\cdot}0$; (a) Notched plane, ……× …… $X/D_e = 0{\cdot}5$; …… □ …… 3·0; ……○…… 5·0; …… △ …… 8·0; …… ⬟ …… 15·0. (b) Unnotched plane. ……× …… $X/D_e = 0{\cdot}5$; …… ■ …… 3·0; …… ● …… 5·0; …… ▲ …… 8·0; …… ⬟ …… 15·0.

that in the unnotched plane there is significant enhancement in shear-layer growth compared to the plain case (Figure 5). However, in the notched plane there is only marginal influence of the notches on the shear-layer growth even though the notches enhance the centreline decay significantly. The enhanced shear-layer growth in the unnotched plane may be taken as an indication of faster cascade of large-scale structures into smaller ones. However, it will be of very high value to authenticate the above observation if visualization with pulsed Schlieren is done on shear layers.

At $20{\cdot}0D_e$, the centreline decay of all the jets slows down and attains an approximately constant value beyond $30.0D_e$ indicating the beginning of the axisymmetric or the fully developed region where the breakdown of large-scale structures initiated at the end of the potential core is completed [19]. The two tab case in a circular nozzle of Zaman *et al.* [9] is included in the plot for the purpose of qualitative comparison with the present work. It is clearly seen that the core length for Zaman *et al.* [9] is the minimum.

3.3. AVERAGE SHOCK-CELL LENGTH

The choked jet-noise and hence the screech frequency are primarily dependent on the length of the shock cells and hence on the strength of the shocks in the shock-cell system [11]. Therefore, the effect of notch on the average length of shock cell, averaged up to four shock cells, was investigated. Figures 7 presents the variation of L_{avg}/D_j versus M_j. Here, L_{avg} is the measured average shock-cell length and D_j the diameter of a fully expanded plain/notched circular-slot jets which was calculated using Tam's relationship [20]

$$\frac{D_j}{D} = \left(\frac{1 + ((\gamma - 1)/2)M_j^2}{1 + ((\gamma - 1)/2)M_d^2}\right)^{(\gamma+1)/4(\gamma-1)} \left(\frac{M_d}{M_j}\right),$$

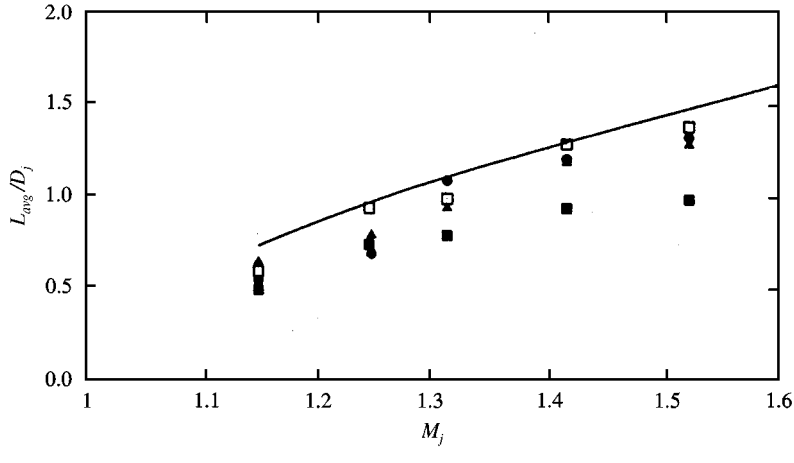

Figure 7. Comparison of average shock-cell length variation with variation in notch geometry. —— Tam's Theory (1988); □ Present work: Plain circle; ▲ Notch: Triangular; ■ Square; ● Semi-circular.

where M_d is the design Mach number of the nozzle. For the slots under study, M_d is obviously 1·0. For comparison, Tam's theory [20] for circular nozzle jets is included. It is seen that the general trend of increasing shock-cell length with M_j is consistent with Tam's theory. The average shock-cell length for plain circle is close to that predicted by Tam's theory though the curve for the present case lies a little below it. For notched cases, a decrease in the average length of shock cell is seen with the curves following the trend of Tam's theory [20] but lying well below the plain case. The reduction in average shock-cell length/spacing in the case of plain circular jets relative to the curve of Tam's theory may be due to the fact that in the case of slot jets, the extremely thin initial boundary layer produces slender vortical structures with very thin cores (thus high vorticity) and with strong azimuthal variations in induced velocity. Hence, the deformation of the vortex structure is speeded up. This, perhaps, leads to faster diffusion of shock cells [21] leading to shorter shock-cell length. The addition of notches speeds up the deformation process further. This perhaps may be the reason for the reduction in the average shock-cell length observed suggesting the existence of a weaker shock-cell system in notched cases relative to the plain circular-slot jet. At $M_j = 1{\cdot}6$, the square notched circular-slot jet shows the weakest of shocks.

3.4. AEROACOUSTIC CHARACTERISTICS

The experimentally observed characteristics of sound radiation from fully expanded (shock-free) and underexpanded (shock-containing) circular-slot jets with and without notches are described in the present section.

3.4.1. *Overall sound pressure results*

Figures 8(a, b) show the OASPL measurements made with the microphone positioned at an observer angle of $\theta = 150^\circ$ to the upstream jet axis and at $R/D_e = 50$ from the slot exit. These values of θ and R/D_e were selected after a detailed survey of the literature [10, 22, 23].

The plain circular-slot jet is seen to radiate higher noise levels relative to notched jets, as seen in Figures 8(a, b). Fluctuation in OASPL values is seen between $M_j = 1{\cdot}2$ and 1·7 after which the values show a definite trend. These fluctuations in OASPL values may be due to the jet oscillations setting in for $1{\cdot}1 < M_j < 1{\cdot}7$ as observed by Hammitt [15] and Sarohia and Massier [24]. These jet oscillations according to Hammitt [15] do not grow uniformly stronger with increasing pressure ratio but reach a peak, fall off, and then rise to a new peak. Since these jet oscillations are directly related to the noise generation in choked jets [10, 23], the radiated noise will have a fluctuating value in this range of M_j, as seen in Figures 8(a, b). Above $M_j = 1{\cdot}7$, the jet seems to stabilize and at $M_j = 2{\cdot}0$, Figure 8(b), relative to plain jet, square notched jet shows a 8 dB reduction followed by triangular and semi-circular cases with 7 and 5 dB reduction, respectively.

The noise levels along the unnotched/minor-axis plane, Figure 8(a), shows a reversal in trend relative to that observed along the major-axis plane, Figure 8(b). At $M_j = 2{\cdot}0$, the semi-circular notched jet shows a minimum noise intensity,

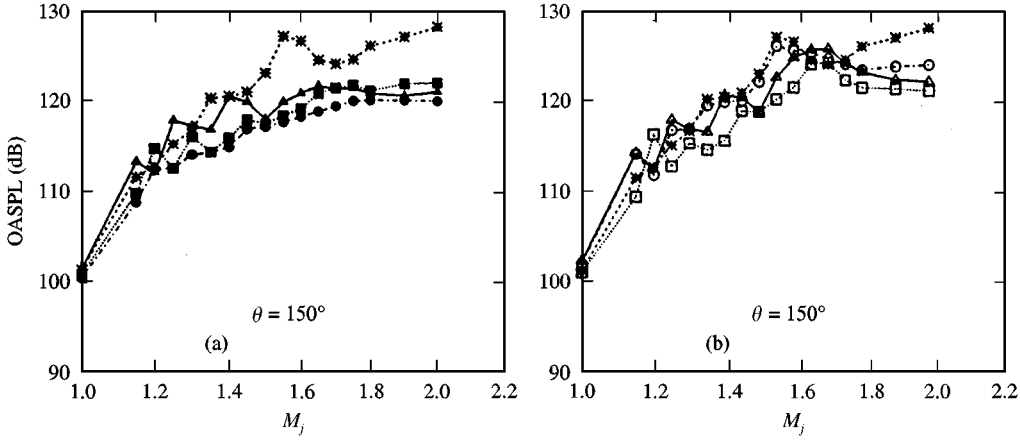

Figure 8(a, b). Overall sound pressure (OASPL) results for the cases investigated with the microphone positioned at 150° to the upstream jet axis and at $R/D_e = 50$ from the jet exit. (a) Minor-axis Plane ·····✱····· Plain circle; ·····■····· Notch: Square; ——▲—— Triangular; -·-·-●-·-·- Semi-circular; $\theta = 150°$. (b) Major-axis plane ·····✱····· Plain circle; ·····□····· Notch: Square; ——△—— Triangular; -·-·-○-·-·- Semi-circular; $\theta = 150°$.

followed by triangular and square cases. This difference in acoustic characteristics between the two planes is typical of non-circular jets where minor-axis sides show lesser noise intensity relative to major plane [22, 25]. Thus, the concept of notched circular-slot jet being considered as an equivalent elliptic jet, as discussed in the preceding sections of mean flow measurements, seems to agree well with the acoustic characteristics of non-circular jets reported in the literature.

Figures 7 and 8 seem to suggest that the notches and their configurations significantly influence the shock development and weaken it resulting in a reduction of OASPL.

3.4.2. *Azimuthal directivity*

It is well known that non-circular jets spread differently in different planes [6, 18, 26] and as such radiate different noise intensities in different planes [27]. The measurements were made starting from the unnotched/minor-axis side, passing through the major-axis side (having the notch) and ending up at the other end of the minor-axis side. The microphone was positioned on a fixed aluminium quadrant, mounted on a tripod stand, and moved in a circular arc at fixed intervals of 10°, $R/D_e = 24$. Figures 9(a, b) show such a plot. At full expansion, as seen in Figure 9(a), plain circle shows maximum noise intensity without any preferred direction as is expected due to symmetry of slot geometry. Notched jets show a significant decrease in noise levels with square notch jet showing minimum value (5 dB decrease) followed by semi-circular and triangular notch jet (3·0 dB). No significant change in noise levels is apparent along the two planes as the flow is not wave-dominated.

In underexpanded conditions, as seen in Figure 9(b), the difference in noise radiated along the two planes of notched jets widens and exhibits trends similar to

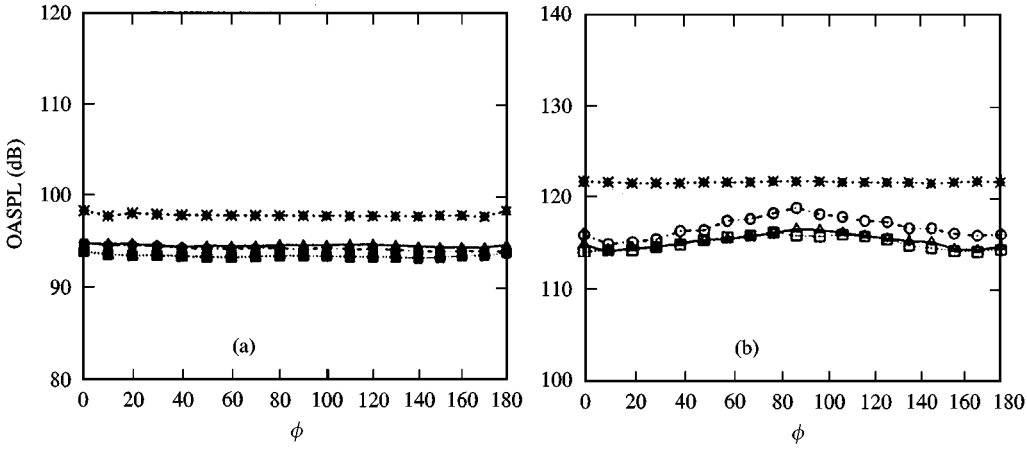

Figure 9(a, b). Plots showing the azimuthal dependence of OASPL for plain and notched circular-slot jets at $M_j = 1{\cdot}5$. (a) $M_j = 1{\cdot}0$ ·····✱····· Plain circle; ·····■····· Notch: Square; ——▲—— Triangular; ----●---- Semi-circular, (b) $M_j = 1{\cdot}5$ ·····✱····· Plain circle; ····· □ ····· Notch: Square; ——△—— Triangular; ----○---- Semi-circular.

those of elliptic jets [25]. The plain circular-slot jet, once again, shows maximum noise levels with no preferred direction. Relative to the plain case, a 6–8 dB reduction is seen in the minor-axis/unmodified plane (absence of notch). As the notch region is approached, a significant increase in OASPL is observed.

3.4.3 *Radial directivity in the aft-qudrant*

Figures 10(a, b) show the angular directivity of jet noise in the aft qudrant. Here, the region defined by $\theta = 0$–90° is referred to as the forward quadrant, and that by $\theta = 90$–180° as the aft qudrant, in accordance with the norms followed by Krothapalli *et al.* [22].

The jets show a clear and distinct noise intensity pattern. It is discernible that the dominant part of the noise is confined in the aft quadrant at angles greater than 100°, whereas for angles less than 100°, the jet noise is low and relatively independent of direction. It is believed [10, 28] that this low-level noise is generated by fine-scale turbulence of the jet flow whereas the dominant part is generated directly by large-scale structures in the jet flow. Relative to the plain circular jet, notched jets show higher noise intensity in both planes for all angles in the aft quadrant. This may be due to the dominance of turbulence structures in notched jets in accordance with the present understanding of turbulent mixing noise of jets [28]. Notch geometry, further, has influence on noise intensity. The triangular notch jet shows a dominance, as was also observed in azimuthal directivity plots, of jet nose followed by the semi-circular and finally, the square case which shows minimum value.

Figures 11(a, b) depict the case of underexpanded (shock-containing) jets at an equivalent Mach number, $M_j = 1{\cdot}5$. It is discernible here, too, that the notch geometry variation has a great influence on the noise radiated along the two planes. The noise intensity is seen to peak at different angles for each notch configuration.

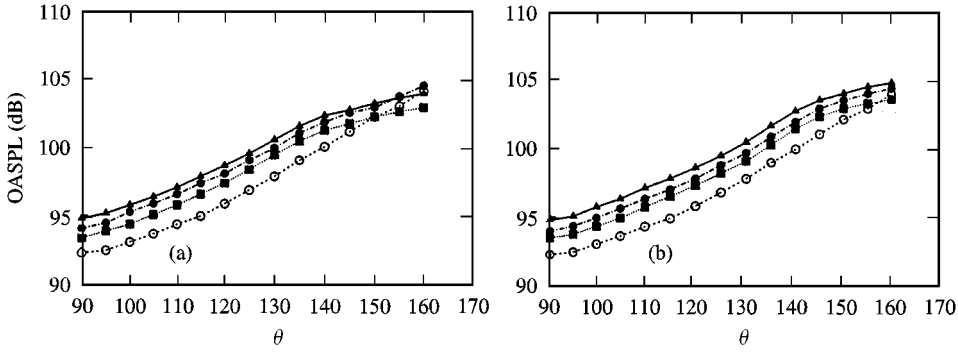

Figure 10(a, b). Plots showing the radial dependence of OASPL in the aft quadrant for plain and notched circular-slot jets as $M_j = 1{\cdot}0$. (a) Minor-axis Plane. (b) Major-axis Plane ····· ○ ·····; Plain circle; ·····■····· Notch: Square; ——▲—— Triangular; ----●---- Semi-circular.

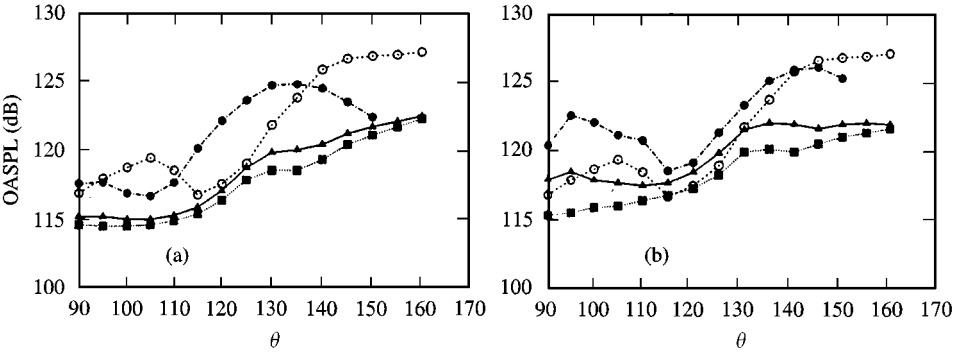

Figure 11(a, b). Plots showing the radial dependence of OASPL in the aft quadrant for plain and notched circular-slot jets at $M_j = 1{\cdot}5$. (a) Minor-axis Plane. (b) Major-axis Plane ·····○·····; Plain circle; ·····■····· Notch: Square; ——▲—— Triangular; ----●---- Semi-circular.

In Figure 11(a), along the minor-axis/unmodified plane at $\theta = 150^\circ$, relative to the plain circular slot jet, the triangular and square notched jets show an approximate reduction of 10 dB. Along the major-axis/modified plane, in Figure 11(b), the Square notched jet, which shows minimum noise levels at all angles, indicates an 11 dB reduction followed by triangular with 10·5 dB and semi-circular with 6 dB reduction.

The above results indicate that the notches significantly influence the shock development process, and hence alter the acoustic fields of these jets. Further, it appears that the sound intensity is relatively dependent upon the notch geometry, and hence the initial jet conditions and shear-layer development.

4. CONCLUSIONS

A passive control of achieving mixing enhancement and noise reduction in circular-slot jets is demonstrated. The results of the experimental investigation are

summarized as follows:

- The presence of a notch in circular-slot geometry makes it slightly non-circular with its major axis along the notched plane. This induces a slight aspect ratio in the otherwise circular geometry causing the modified circular jet to switch axis like any other non-circular geometry. This process induces higher mixing in notched cases.
- The variation of average shock cell length of both plain and notched jets with fully expanded jet Mach number, M_j, follows the trend predicted by Tam. The shorter average shock-cell lengths for notched cases relative to plain case suggests a weaker shock-cell system in notched circular-slot jets. Further, different notch configurations show different average shock-cell lengths indicating that the notch geometry greatly influences the shock-cell development for underexpanded conditions.
- The notched circular-slot jets show significantly reduced noise levels relative to plain jet. It may, therefore, be suggested that the reduction in the magnitude of OASPL is due primarily to the weaker shock-cell structure in notched/modified jets.
- The modified circular-slot jet radiates noise like a typical non-circular jet with a higher noise intensity along the major-axis/modified plane, and a lower one along the minor-axis/unmodified plane.

REFERENCES

1. E. Gutmark, and K. C. Schadow, 1988 *Experiments in Fluids* **6**, 129–135. Selective flow control in triangular jets.
2. G. F. Marster, 1981 *AIAA Journal* **19**, 148–152. Spanwise velocity distribution in jets from rectangular slots.
3. W. R. Quinn, 1994 *AIAA Journal* **32**, 547–554. Development of a large aspect-ratio rectangular free jet.
4. R. W. Wlezien and K. Kibens, 1988 *AIAA Journal* **26**, 27–33. Influence of nozzle asymmetry on supersonic jets.
5. M. H. Steiger, P. M. Sforza, and N. Trentacoste, 1966 *AIAA Journal* **4**, 800–806. Studies in three-dimensional viscous jets.
6. A. K. M. F. Hussain, and H. S. Hussain, 1989 *Journal of Fluid Mechanics* **208**, 257–320. Elliptic jets Part I: characteristics of excited and unexcited jets.
7. W. R. Quinn, 1988 *Physics of Fluids* **31**, 1017–1025. Experimental and numerical study of a turbulent free square jet.
8. L. J. S. Bradbury, and A. H. Khadem, 1975 *Journal of Fluid Mechanics* **70**, 801–813. The distortion of a jet by tabs.
9. K. B. M. Q. Zaman, M. Samimy, and M. F. Reeder, 1993 *AIAA Journal* **31**, 609–619. Effect of tabs on the flow and noise field of a axisymmetric jets.
10. H. K. Tanna, 1977 *Journal of Sound and Vibration* **50**, 429–444. An experimental study of jet noise, Part II: shock-associated noise.
11. T. D. Norum, 1983 *AIAA Journal* **21**, 235–240. Screech suppression in supersonic jets.
12. Y. Hsia, D. Bagdanoff, A. Krothapalli, and K. Karamcheti, 1986 *Journal of Sound and Vibration* **106**, 119–143. Role of screeching tones in the mixing of an underexpanded rectangular jet.
13. S. S. Pannu, and Johanassen. 1976 *Journal of Fluid Mechanics* **74** (Part 3), 515–528. The structure of jets from notched nozzles.

14. J. McDaniel, A. Krothapalli, and D. Bagdanoff, 1990 *AIAA Journal* **28**, 2136–2138. Effect of slotting on the noise of an axisymmetric supersonic jet.
15. A. G. Hammitt, 1961 *Journal of Aerospace Sciences* **28**, 673–680. The oscillations and noise of an overpressure sonic jet.
16. D. R. Glass, 1968 *AIAA Journal* **6**, 1890–1897. Effects of acoustic feedback in the spread and decay of supersonic jets.
17. A. K. M. F. Hussain, and V. Ramjee, 1976 *Transactions of the ASME, Journal of Fluids Engineering* **98**, 58–59. Effects of axisymmetric contraction shape on incompressible turbulent flows.
18. E. Gutmark, and K. C. Schadow, 1987 *Physics of Fluids* **30**, 3448–3454. Flow characteristics of orifice and tapered jets.
19. A. Roshko, 1976 *AIAA Journal* **14**, 1349–1357. Structure of turbulent shear flows: a new look.
20. C. K. W. Tam, 1988 *Journal of Sound and Vibration* **121**, 135–147. The shock-cell structures and screech frequency of rectangular and nonaxisymmetric supersonic jets.
21. C. K. W. Tam, and D. E. Burton, 1984 **138**, 249–295. Sound generated by instability waves of supersonic flows. Part I, two-dimensional mixing layers. Part II, Axisymmetric jets.
22. A. Krothapalli, D. Washington, C. J. King, F. S. Alvi, 1996 *AIAA Journal* **34**, 1562–1569. Aeroacoustic properties of a supersonic diamond-shaped jet.
23. M. K. Ponton, and J. M. Seiner, 1992 *Journal of Sound and Vibration* **154**, 531–549. The effects of nozzle exit lip thickness on plume resonance.
24. V. Sarohia, and P. F. Massier, *AIAA Journal* **16**, 831–835. Experimental results of large-scale structures in jet flows and their relation to jet noise production.
25. S. B. Verma, and E. Rathakrishnan, 1998 *AIAA Paper No AIAA-98-3258,* 34*th AIAA/ASME/SAE Joint Propulsion conference*, 13 *July*, *OH*, *U.S.A.* Mixing benefit and noise characteristics of notched elliptic-slot jets.
26. E. Gutmark, and C. M. Ho, 1987 *Journal of Fluid Mechanics* **179**, 383–405. Vortex induction and mass entrainment in a small aspect ratio elliptic jet.
27. K. C. Schadow, C. J. Bicker, E. Gutmark, *Experiments in Fluids* **28**, 1163–1170. Near acoustic field and shock structure of rectangular supersonic jets.
28. S. B. Verma, and E. Rathakrishnan, 1998 *International Journal of Turbo and Jet Engines* **15**, 7–25. Noise attenuation and enhanced mixing in notched elliptic-slot jets.
29. P. Chen, J. M. Seiner, C. K. W. Tam, 1992 *AIAA Journal* **30**, 1747–1752. Relationship between instability waves and noise of high speed jets.